The relationship between temporal phase discrimination ability and the frequency doubling illusion

Kunjam Vallam

Department of Optometry & Vision Sciences, The University of Melbourne, Carlton, Victoria, Australia, & ARC Centre of Excellence in Vision Science, School of Psychology, The Australian National University, Canberra, Australia

Andrew B. Metha

Department of Optometry & Vision Sciences, The University of Melbourne, Carlton, Victoria, Australia

The frequency doubling illusion (FDI) occurs when a low spatial frequency sinusoidal grating is modulated at high temporal frequencies—its apparent spatial frequency increases. A recent study suggests that this illusion is perceived due to a frequency-dependent loss of temporal phase encoding ability. We sought to elucidate the relationship between temporal phase encoding and the FDI by exploring the spatiotemporal characteristics of temporal phase discrimination (TPD) thresholds using a novel stimulus comprising three grating patches presented simultaneously in a triangular pattern. A reference grating was presented superiorly, and six degrees below two gratings (one a copy of the reference) were each randomly presented in one of two fixed positions. The odd grating had abutting regions of spatial half-cycles with alternate half-cycles locked in temporal phase. The temporal phase difference between adjoining half-cycles was varied between 0° and 180° via QUEST staircase—subjects had to identify which lower stimulus appeared different from the reference grating. TPD thresholds were measured for 0.25, 0.50, and 2.20 cpd stimulus at six temporal frequencies (1 to 28 Hz) at 2×, 4×, and 8× orientation identification contrast thresholds. For all subjects, thresholds were variable at low contrasts. At higher contrasts, TPD thresholds increase for 0.25 and 0.50 cpd gratings with increasing flicker rate. These data support the idea that frequency-dependent loss of temporal phase encoding ability could possibly underlie the FDI.

Keywords: illusion, frequency doubling, temporal phase, discrimination, spatial models

Citation: Vallam, K., & Metha, A. B. (2007). The relationship between temporal phase discrimination ability and the frequency doubling illusion. *Journal of Vision, 7*(14):17, 1–11, http://journalofvision.org/7/14/17/, doi:10.1167/7.14.17.

Introduction

The spatial frequency doubling illusion (FDI) occurs when the contrast of a low spatial frequency sinusoidal grating is modulated at high temporal frequencies—its apparent spatial frequency increases (Kelly, 1966). Maddess and Henry (1990, 1992) suggested that the illusion arises due to the transduction properties of a specific class of magnocellular ganglion cells, M(y) cells, which resemble cat Y cells in their non-linear spatial summation response characteristics (Blakemore & Vital-Durand, 1986; Kaplan & Shapley, 1982; Marrocco, McClurkin, & Young, 1982; Shapley, Kaplan, & Soodak, 1981). However, this notion is contentious since several studies have reported that in both macaque retina and LGN, there are very few magnocellular ganglion cells that demonstrate the required non-linearity in spatial summation (Derrington & Lennie, 1984; Kaplan & Shapley, 1986; White, Sun, Swanson, & Lee, 2002). White et al. (2002) specifically demonstrated that magnocellular ganglion cells have very low non-linearity indices and are not capable of generating the sort of non-linear responses required to explain the FDI, especially at the low spatial frequencies for which the illusion is seen. To explain the perception of this illusion, White et al. proposed a new theory whereby spatial frequencies appear doubled in the FDI because at high temporal frequencies we lose our ability to precisely encode the timing of light modulations, i.e., the change from one luminance polarity to the other occurs so fast that we see both the polarities simultaneously and it gives the perception of doubled frequency. Nevertheless, their physiological measurements from magnocellular ganglion cells showed that these cells can adequately encode temporal phase of the fast flickering gratings; hence, the locus of any psychophysically identified loss of temporal phase encoding must be due to more central limitations on visual information processing.

While this theory is successful in explaining the perception of doubled frequencies in the FDI, it fails to explain why the FDI is perceived only for low spatial

doi: 10.1167/7.14.17 Received September 24, 2006; published December 20, 2007 ISSN 1534-7362

frequencies. To examine the spatiotemporal relationship between the FDI and loss of temporal phase encoding, in this study we measured the temporal phase discrimination (TPD) thresholds over a range of spatiotemporal parameters. To measure the temporal phase encoding ability, we modified the stimulus paradigm used by White et al. (2002). Their stimulus consisted of two sets of horizontal grating pairs with 30′ separations between the gratings in each grating pair. In one grating pair, both gratings were locked in phase but in the other grating pair, gratings were flickering at 180° temporal phase difference. With this stimulus, they psychophysically measured the contrast thresholds for discriminating a pair of flickering grating locked in phase from a pair of flickering grating at opposite temporal phase. Recent reports suggest that the TPD thresholds are affected significantly if the two targets are separated by a spatial gap (Forte, Hogben, & Ross, 1999; Victor & Conte, 2002), so it is likely that the TPD thresholds measured by White et al. may be artificially elevated because of the 30′ gap between their gratings.

To circumvent this problem, we adopted the stimulus used by Mechler and Victor (2000) (with modifications—explained below) which consisted of two horizontally oriented gratings with similar spatiotemporal configurations except that the temporal phase of one grating was advanced. These gratings were placed adjacent to each other so that there was a temporal phase offset across the edge, which observers had to identify. As there is no separation of the gratings, this kind of stimulus design is an advantage over White et al.'s (2002) stimulus design. But, as Mechler and Victor accepts, observers found this task difficult (due to only one edge between the two regions) and required extensive practice to acquire a reliable cue. They could perform the task only because of the apparent motion cue across spatially aligned abutting horizontal gratings.

To avoid this motion cue, we modified the stimulus design used by Mechler and Victor (2000) and generated a novel stimulus (explained below). Our stimulus design had two main advantages. Firstly, the phase offset could be varied to any value in the range of 0° to 180° while White et al. (2002) could only use 180° phase offset. (In this kind of task, the experimental parameter (phase-offset) can only vary between 0° and 180° as temporal cycle repeats itself in reverse order after 180° and thus 180° is the upper bound to phase offset thresholds.) Secondly, TPD thresholds could be measured at any contrast level whereas White et al. were limited to measuring the contrast required to discriminate temporal phase offset of only 180° between flickering grating pairs.

With our stimulus design, we could characterize the temporal phase encoding for each spatial and temporal frequency at higher multiples of contrast threshold levels (measured as the contrast required to identify orientation of the sinusoidal gratings—orientation identification thresholds). Our results show that the loss of temporal phase encoding ability is dependent on the spatial and temporal frequency of the flickering gratings and only occurs principally at those spatiotemporal parameters associated with the appearance of the FDI.

General methods

Apparatus and observers

Stimuli were presented on a 37 cm × 28 cm (1024 × 768 pixels) Mitsubishi Black Diamond Monitor running at 85 Hz with background luminance set to 75 cd/m^2. The screen luminance was linearized with Photo Research-650 SpectraScan Colorimeter and controlled with 10-bit accuracy by ATI Radeon video card (via OpenGL) installed in a Macintosh G4 computer running EXPO software.

Six observers with normal corrected visual acuities participated in these experiment. Observers viewed the monitor screen with preferred eye at a viewing distance of 57 cm in dim ambient lighting conditions with unrestrained heads and normal pupils (each pixel subtended 0.036° at 57 cm viewing distance). All observers were pre-presbyopic (mean age: 26.1 ± 5.93 years) and wore their habitual refractive correction during testing. The non-tested eye was covered with a uniform translucent patch to avoid binocular rivalry. Two of the six subjects (KV, AM) were aware of the purposes of the experiments and the other four subjects (MD, PB, CA, YL) were naïve. All procedures were carried out in accordance with NHMRC guidelines for human observers and were approved by the Department of Optometry and Vision Sciences Ethics Committee, which is based on the tenets of the Declaration of Helsinki. All observers gave informed written consent prior to participation in the study.

Stimuli and procedure

The stimuli consisted of counterphase flickering sinusoidal gratings. They were presented in a spatially smoothed Gaussian window to band-limit their spatial frequency content. The luminance distribution of the stimuli as a function of space (x) and time (t) can be described mathematically as

$$I(x,t) = I_{\text{mean}}\{1 + C \cdot \mathrm{G}(x,t) \cdot L(x,t)\}, \quad (1)$$

where I_{mean} is the mean intensity level; C is the contrast modulation (in percent Michelson contrast) generated by equally modulating red, green, and blue guns of the CRT

monitor; and $L(x,t)$ is the grating function. Two grating functions were used, expressed mathematically as

$$L(x,t) = \sin(2\pi f_x x + \phi_s) \cdot \sin(2\pi f_t t + \phi_t), \quad (2)$$

$$L(x,t) = \sin(2\pi f_x x + \phi_s) \cdot \sin(2\pi f_t t + (\phi_t + \Delta_t)), \quad (3)$$

where f_x is the spatial frequency (cpd); f_t is the temporal frequency (Hz); and ϕ_s and ϕ_t are spatial and temporal offset phases (radians). As shown above, two gratings were exactly similar except that the temporal phase of second grating was advanced by Δ_t.

$G(x,y,t)$ is the Gaussian window function and describes how the contrast envelope changes over space and time. Mathematically it can be expressed as

$$G(x,y,t) = e^{-\left(\frac{(x-x_0)^\alpha}{2\sigma^2}\right)} \cdot e^{-\left(\frac{(y-y_0)^\alpha}{2\sigma^2}\right)} \cdot \sin(2\pi f_t t), \quad (4)$$

where x (or y) is the position in space and x_0 (or y_0) is the centre position in degrees. In the current experiments, standard deviation (σ) was 2.8° and exponent (α) was 4 so that greater number of grating cycles were visible through the window. The orientation of a stimulus specified here is such that 0° refers to grating bars or lines that are elongated horizontally. Other angles indicate bar or line elongation rotated counter clockwise relative to horizontal.

Three spatial frequencies (0.25, 0.50, and 2.20 cpd) and six temporal frequencies (1, 5, 10, 15, 21, and 28 Hz) were explored. Each experimental session had only one spatial frequency with two temporal frequencies randomly interleaved. To reduce the impact of any slow variation in sensitivity over time, TPD thresholds were measured immediately after the determination of contrast thresholds.

Orientation identification thresholds: The stimuli consisted of counterphase flickering sinusoidal gratings (generated from Equations 1.1 and 1.2). All presentations were made in the centre of the monitor in a 12° diameter spatially smoothed Gaussian window (Equation 1.4). In each trial, orientation of the gratings was randomized to either 45° or 135°; spatial phase was randomly varied to any value between 0° and 360° and temporal phase was preset at 0°. Each trial consisted of two temporal intervals (raised cosine window) of 1000 ms with 500 ms interstimulus interval. The onset of each stimulus interval was accompanied by an audible beep.

Within each trial, gratings were presented either in the first or second interval while a blank at the background mean luminance appeared in the other. Observers indicated orientation of the gratings by key presses. This 2-interval forced choice procedure was combined with the method of constant stimuli (MoCS) task with 5 contrast levels. Twenty-five trials were presented at each contrast level during each experimental session. During a given session the different stimulus intensity levels were visited in pseudo-random order: Each intensity level was presented once in random order until they had all been presented before the sequence began again, this time in a different order.

Temporal phase discrimination thresholds: A novel stimulus was used for the measurement of TPD thresholds. Specifically, two vertically oriented counterphase flickering sinusoidal gratings were generated, say gratings A and B. Spatial and temporal characteristics of both gratings were exactly similar except that the temporal phase (ϕ_t) of grating A was 0° (generated from Equation 1.2) and grating B had a variable (Δ_t) added to the temporal phase of grating A ($\phi_t + \Delta_t$) (generated from Equation 1.3). Then spatial half-cycles of each grating were separated (Figures 1A and 1B) and used to generate a new grating (C). This grating C had abutting regions of grating half-cycles with alternate half-cycles taken alternately from gratings A and B. First half-cycle of grating C was taken from grating A, second half-cycle from grating B, third half-cycle again from grating A, and hence forth (Figure 1B). Now this grating C is similar to the original grating A except that every alternate half-cycle is temporally advanced by Δ_t. The number of half-cycles in grating C was always an even number and equal to those in grating A.

Stimulus display consisted of three grating patches (each in a 12° diameter spatially smoothed Gaussian circular window) presented simultaneously around the centre of display monitor (see Figure 2A). The presentation was done in a raised cosine window of 2000 ms to reduce transients at the beginning and end of a presentation. The onset and offset of each stimulus interval were accompanied by two different audible beeps. Fixation marks were always present in the centre of each grating patch and subjects could freely move their eye. In a trial, all three gratings were vertically oriented and flickered at the same temporal frequency.

The grating presented at the top of the triangular pattern was a reference grating (grating A in Figure 2A). And beneath it two gratings, one exactly a copy of the reference grating (grating B), and a composite grating (grating C) were randomly presented in either of the lower two positions. As explained above, the composite grating was generated by placing abutting regions of grating half-cycles so that each alternate half-cycle was advanced by Δ_t temporal phase compared to its direct neighbor. Figure 2B shows three examples of composite grating with Δ_t of 45°, 90°, and 180°. Five frames of a temporal cycle are shown with their respective contrast profiles. Three similar stimuli were created: one each for 0.25, 0.50, and 2.20 cpd.

At each trial, subject's task was to identify the grating (among the lower two grating patches) that was different from the reference grating, i.e., to identify the composite grating C. Specifically, the instructions were "Which of the lower two gratings is different from the upper reference grating?" The composite grating was similar to

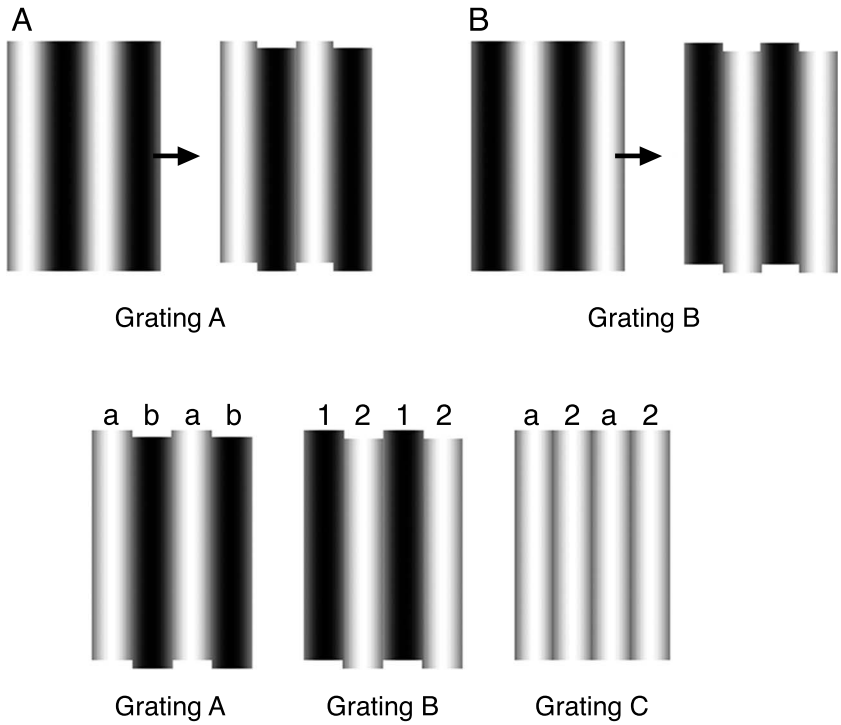

Figure 1. Generation of grating C from A and B. "Freeze-frame" of four half-cycles of each grating are shown. (A) Grating A is generated from Equation 1.2 using $\phi_t = 0°$ and half-cycles are separated. (B) Grating B is generated from Equation 1.3 using $\phi_t = 0°$ and $\Delta_t = 180°$ and half-cycles are separated. (C) Alternate half-cycles from gratings A and B are placed adjacently and a new grating C is generated. Please note that the alternate half-cycles are vertically displaced for clarity purpose only. In the actual stimulus, all half-cycles are vertically aligned as shown in Figure 2A.

other two gratings in all aspects, except a temporal phase offset (Δ_t) between the alternate half-cycles. This two-alternative forced choice (2-AFC) procedure was combined with an adaptive QUEST staircase, which controlled Δ_t. The range of Δ_t was fixed between 0° and 180°. For each observer, starting value of Δ_t for each spatial and temporal frequency was determined from pilot experiments performed immediately before. TPD thresholds were measured at set multiples (2×, 4×, and 8×) of orientation identification threshold contrast levels. Prior to data collection, subjects were given sufficient practice on the task to ensure that any perceptual learning effect had stabilized and thus would not influence the results. All subjects found the task difficult to perform at low contrast levels. For the 2.20-cpd composite stimulus, they reported an overall apparent brightness increase of the composite stimulus at high temporal frequencies. This issue is discussed further in the Discussion section.

Analyses

A similar analytical procedure was used to obtain threshold values for both the contrast threshold experiment (using MoCS) and the TPD experiment (using QUEST staircase). Responses from an experimental session were pooled at each absolute level of the MOCS/QUEST and a cumulative normal psychometric curve was fitted to the proportion of correct responses by minimizing chi-square, a statistic describing the difference between the raw data and fitted curve. All function fitting was performed using Matlab (version 5.2.1, The Mathworks, Inc.). Threshold was taken as the mean of the fitted cumulative normal, i.e., at the 75% correct performance level. The 95% confidence intervals on the threshold estimate were obtained by bootstrapping the original data sets (Efron & Tibshirani, 1998). Occasionally, in the TPD experiment, the data were noisy and the data-fitting program failed to supply sensible thresholds. Such thresholds were discarded and rest of the results were averaged to identify group performance.

Figure 3 shows a sample psychometric function plotting proportion correct responses in orientation identification task (open squares) and TPD thresholds (filled circles) against log contrast. The smooth curve for orientation identification task is a cumulative normal function gradually increasing from chance to 100% performance levels. The contrast level for 75% correct was taken as contrast threshold. Once this contrast

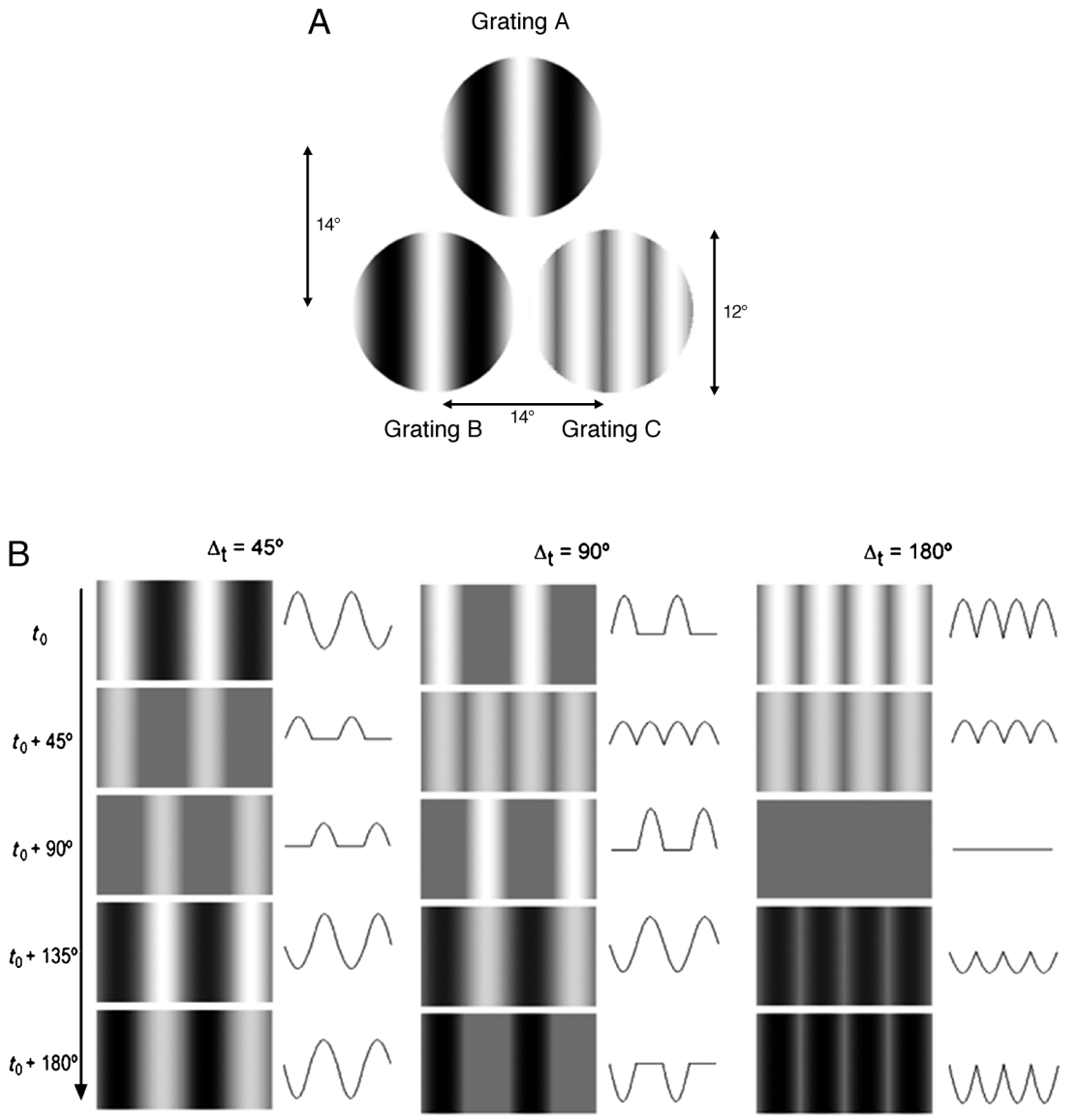

Figure 2. Illustration of the stimulus used for measuring the TPD thresholds. (A) Stimulus display showing three grating patches: Grating A is the reference grating, Grating B is an exact replica of the reference grating, and Grating C is the composite grating generated by placing abutting regions of grating half-cycles. Every alternate half-cycle in grating C is advanced by 180° (Δ_t) temporal phase (see text for detail). Separation between the centre of gratings and grating sizes are shown. (B) Three examples of composite grating C with Δ_t of 45°, 90°, and 180° showing five frame each with their respective contrast profiles. The frames are separated in time (for illustrative purposes only) so that each successive frame indicates 45° step of a temporal cycle. t_0 indicates start of a temporal cycle. This illustration shows two spatial cycles in each grating patch in hard-edged windows but in experiment, circular windows were used with Gaussian envelope. Not drawn to scale.

threshold was established for each observer, TPD thresholds were measured at 2×, 4×, and 8× contrast threshold level.

Results

Figures 4, 5, and 6 shows temporal frequency-dependent TPD thresholds for each subject for 0.25, 0.50, and 2.20 cpd TPD stimulus at two contrast levels (4× and 8× orientation identification contrast threshold—each shown with different symbols and pattern of lines).

Each subject reported that the task was difficult at lowest contrast level and were unable to reliably identify the composite grating among the lower two gratings in the stimulus. In such situations, subjects gave noisy results and adaptive staircase did not converge. Hence, results for the 2× contrast threshold are not shown. As contrast level increased, subject's performance and reliability improved. At higher contrast levels, at few frequencies, observers

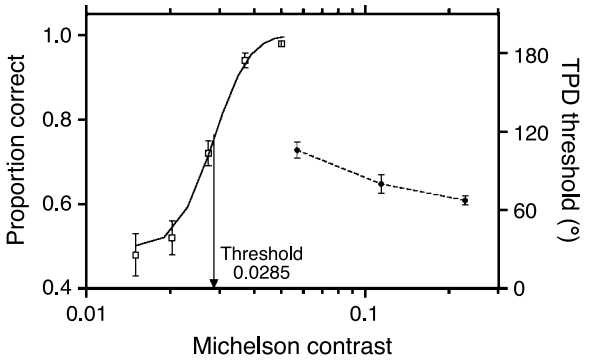

Figure 3. Sample psychometric function showing proportion correct responses in orientation identification task (open squares) and TPD thresholds (filled circles) against Michelson contrast. Error bars on orientation identification responses indicate SEMs (estimated from binomial distribution) and on the TPD thresholds indicate 95% CIs (estimated from bootstrapping procedure). The cumulative normal function for contrast threshold measurement is shown as smooth continuous line. These are the results of a typical observer for 0.25 cpd grating, counterphase flickering at 10 Hz. TPD thresholds were measured at 2×, 4×, and 8× orientation identification contrast threshold levels.

could not give reliable results and no thresholds were available. We believe that this information is necessary and indicates the difficulty of the task at selected spatiotemporal parameters. Such data points are shown in the upper part of the graphs with similar symbols as those used for the data points for which reliable results were obtained.

For the 0.25-cpd TPD stimulus, all observers found the task more difficult for high temporal frequencies. At low temporal frequencies, the instantaneous luminance polarity of each bar of the sinusoidal grating could be identified with assurance and TPD thresholds were low, approximately 30–40° (see average results in Figure 6). At high temporal frequencies, gratings appear to have shimmery appearance in which the specific luminance polarity of each grating bar was not easily discernible, and hence the composite grating could not be identified even at the maximum temporal phase offset. Figure 3 shows that the TPD thresholds approach upper bound (180°) at 20 Hz. Two subjects (PB and KV) found the task difficult at highest contrast levels also.

Figure 5 shows temporal frequency-dependent TPD thresholds for each subject for 0.50 cpd TPD stimulus. In comparison to the task for 0.25 cpd stimulus, at 4× and 8× contrast threshold levels subjects found the task easier for 0.50 cpd stimulus. Results show that at low temporal frequencies, TPD thresholds were low, approximately 30–40°, but as the temporal frequency increases, TPD thresholds increases, and approaches a maximum of approximately 90° for each subject.

A different trend is seen with the 2.20 cpd gratings (see Figure 5). For all subjects, TPD thresholds have larger error bars at the low temporal frequencies (1 and 5 Hz) and then improve at 15 Hz and remain at approximately 50° until 28 Hz. The contrast-dependent difficulty in performance noticed earlier is now observed only at the low temporal frequencies. Figure 6 shows that the data points for which no data was available are more frequent for low temporal frequencies than at high temporal frequencies.

The average results of all subjects (whenever reliable thresholds were obtained) are shown in Figure 7. These results show that for the low spatial frequency TPD stimulus, TPD thresholds increase as the flicker frequency increases. However, this temporal frequency-dependent loss of temporal phase encoding reduces as the spatial frequency of the stimulus increases and at the highest spatial frequency (2.20 cpd) of the experiment, temporal phase encoding is significantly improved.

Discussion

Our experiments show that the task of temporal phase encoding of counterphase flickering gratings is contrast dependent for all spatial and temporal frequencies. At high contrast levels, all observers can encode temporal phase of a 0.25-cpd test grating at low temporal frequencies but as the temporal frequency increases, temporal phase encoding becomes impossible. Notably, at the spatiotemporal parameters germane to the FDI (low spatial frequencies counterphase modulating at high temporal frequencies), loss of temporal phase encoding is maximal. Overall, if temporal phase encoding is present, thresholds for the 8× contrast level are lower than thresholds for the 4× contrast level for all spatial and temporal frequencies. At 2× orientation identification contrast threshold levels, subjects found the task difficult but this performance-related variability reduces as contrast levels are increased.

In addition, we also observed that the thresholds of temporal phase encoding improve significantly for the 2.20-cpd stimulus. Similar results are also evident in the results of White et al. (2002). Their Figure 6 shows that the temporal phase encoding thresholds improve as the spatial frequency is increased from 0.20 to 1.00 cpd. They did not provide an explanation for this spatial frequency-dependent improvement in the temporal phase encoding. Using the current understanding of temporal phase encoding ability, an explanation is offered below as to why we observed improvement in the TPD thresholds at high spatial frequencies.

The temporal frequency-dependent loss of temporal phase encoding ability has also been suggested in the studies related to figure-ground discrimination (Forte et al., 1999; Lee & Blake, 1999a, 1999b; Leonards, Singer, & Fahle, 1996; Rogers-Ramachandran & Ramachandran,

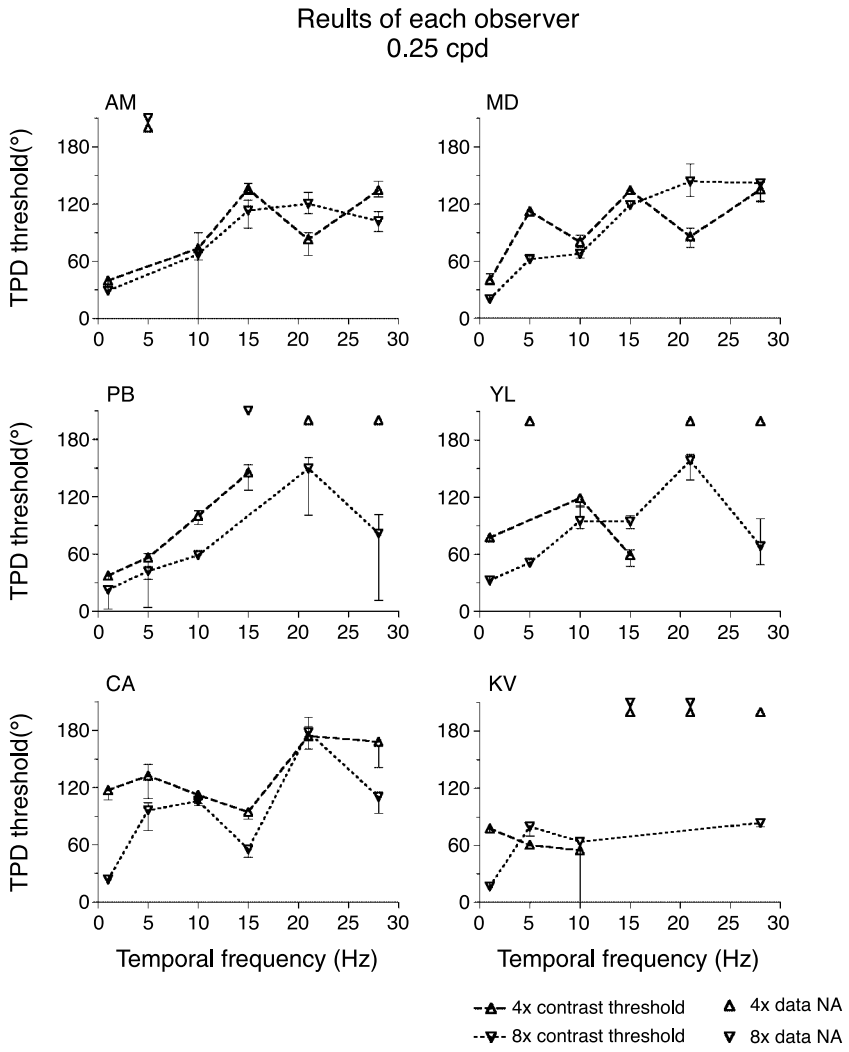

Figure 4. TPD thresholds obtained from 0.25 cpd TPD stimulus plotted against the temporal frequency for each subject. Thresholds at three contrast levels are shown with different symbols and pattern of lines. Data points for which threshold measurements were not available are shown in the upper part of the graphs with similar symbols as those used for the data points for which reliable results were obtained. Error bars indicate 95% CI derived by bootstrapping the original data set.

1998). These studies utilize non-sinusoidal stimuli like geometric targets flickering on a uniform background and they change the temporal phase relationship between the target and background to identify the role of temporal phase in discriminating figure from the background. These studies report that as the temporal frequencies of the flickering target increases, surface characteristics (e.g., color or texture) of the target and background disappear due to loss of temporal phase encoding. Despite this, the visual system can segregate a visual scene into separate target and background regions based only on the temporal phase differences, i.e., the "temporal cues." At high temporal frequencies, under optimal conditions, a target can be segregated from the background at the temporal phase difference of 6–7 ms (Fahle, 1993). These low thresholds translate into temporal phase offsets of approximately 60° for the visual stimuli using sinusoidal gratings in our experiments.

Kojima (1998) investigated the role of spatial frequency in figure/ground segregation task based on temporal phase differences. He used three types of random dot textured patterns—unfiltered random dot pattern, low-pass filtered patterns, and high-pass filtered patterns. Their results show that performance of the subjects improves as spatial frequency of the stimulus is increased. For the high-pass filtered patterns, temporal phase thresholds were 13.3 ms (lowest possible with their experimental set up) whereas for the low-pass filtered patterns, thresholds were approximately 70 ms. They explained these results by proposing that both the spatial and temporal information complement each other in the figure/ground segregation task. If spatial information in the visual display is increased by

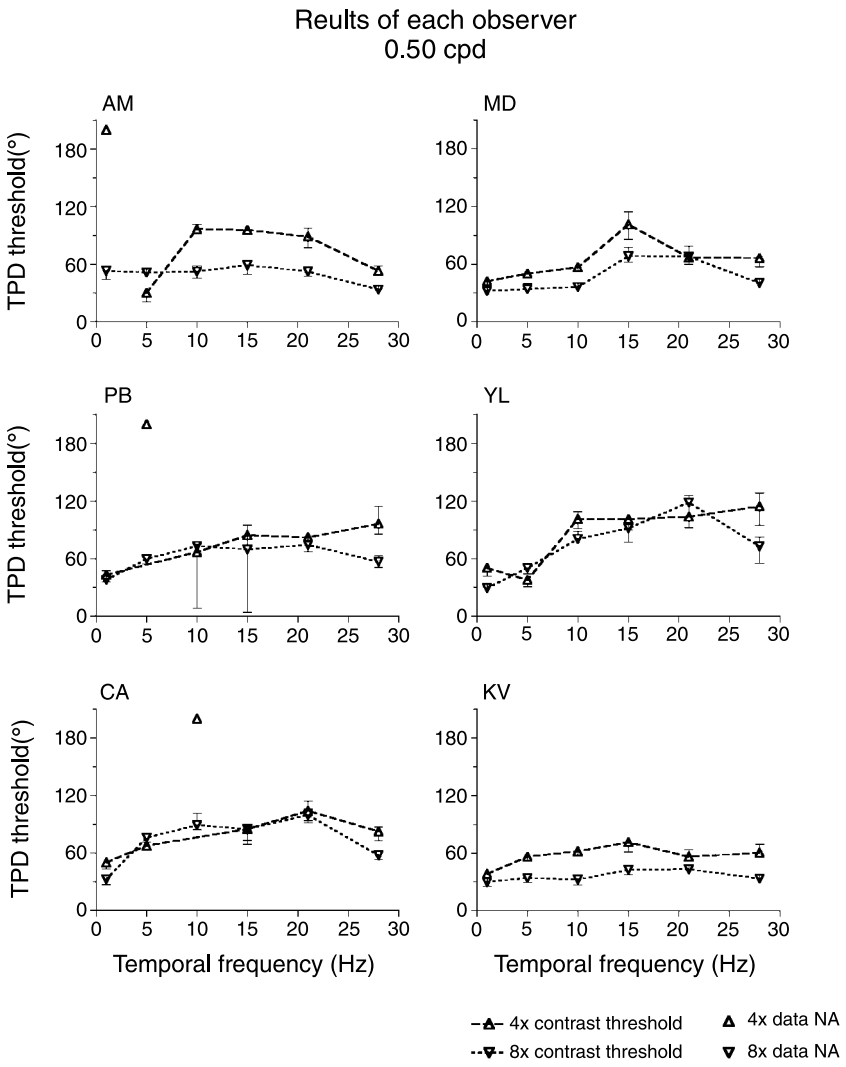

Figure 5. TPD thresholds obtained from 0.50 cpd TPD stimulus plotted against the temporal frequency for each subject. Thresholds at three contrast levels are shown with different symbols and pattern of lines. Data points for which threshold measurements were not available are shown in the upper part of the graphs with similar symbols as those used for the data points for which reliable results were obtained. Error bars indicate 95% CI derived by bootstrapping the original data set.

using high spatial frequency stimulus then the thresholds for temporal parameter can be very low. In the vernier task, Mechler and Victor (2000) came to a similar conclusion. They showed that the vernier thresholds are lower for drifting gratings than for flickering gratings; suggesting that the spatiotemporal context is critical in precise temporal assessment, temporal information alone is not sufficient.

In a flickering sinusoidal grating, zero-crossings of the flickering grating provide strong spatial cues (White et al., 2002). As the spatial frequency of the grating increases, the number of zero-crossings per degree of visual angle also increases which increases the amount of spatial cues present in the grating. As a result, temporal phase encoding at high temporal frequencies should improve, as observed by White et al. (2002) and in the current study. This improvement in the temporal phase encoding can explain the results of several studies that have reported that the FDI disappears at the high spatial frequencies (Kelly, 1966; Parker, 1983).

While performing the TPD task for 2.20 cpd stimulus, our observers reported that the composite grating appear brighter at approximately 15–28 Hz. Each subject reported that this apparent brightness is visible only when the temporal phase offset is above threshold. It is likely that at these parameters another mechanism is stimulated which gives rise to this apparent brightness. To further investigate the issue of apparent brightness, we performed Fourier analysis of the composite grating of our stimulus with different values of Δ_t at several time-points in a temporal cycle. Our analysis showed that as the value of Δ_t increases from 0° to 180°, average energy in a

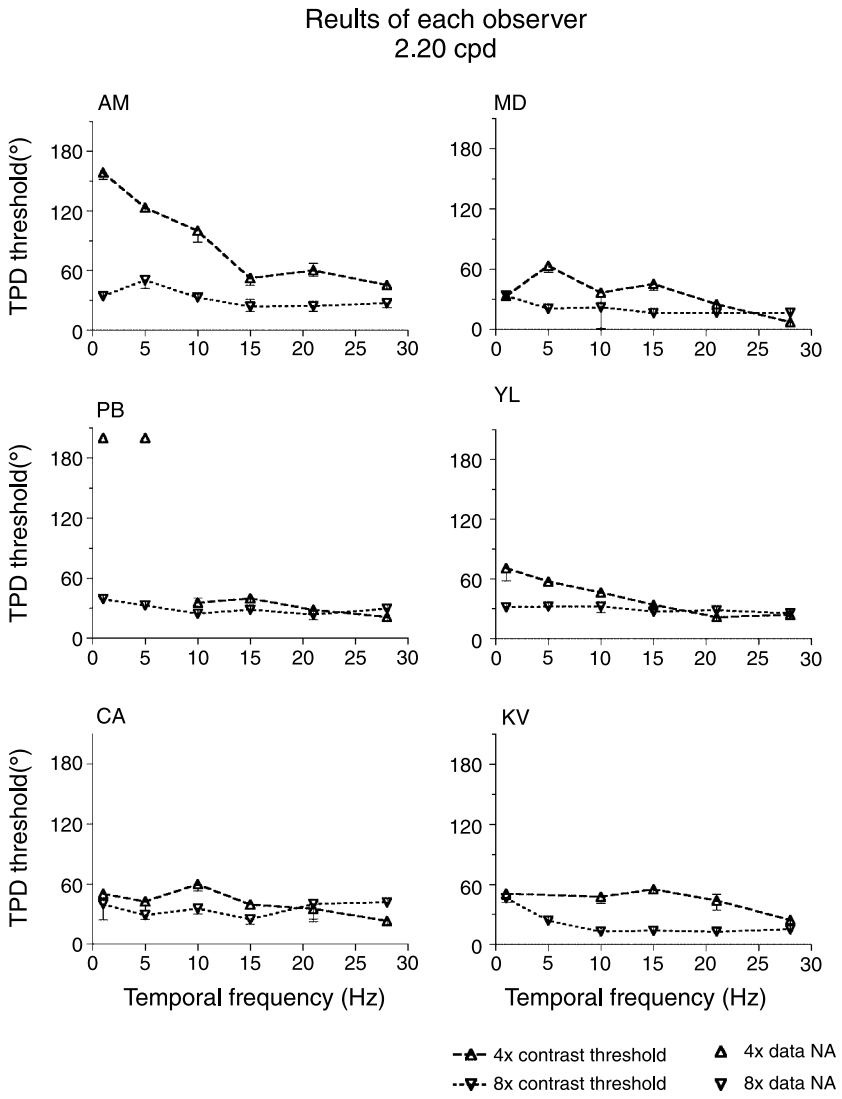

Figure 6. TPD thresholds obtained from 2.20 cpd TPD stimulus plotted against the temporal frequency for each subject. Thresholds at three contrast levels are shown with different symbols and pattern of lines. Data points for which threshold measurements were not available are shown in the upper part of the graphs with similar symbols as those used for the data points for which reliable results were obtained. Error bars indicate 95% CI derived by bootstrapping the original data set.

temporal cycle shifts from its nominal spatial frequency (for example, 0.25 cpd) to doubled spatial frequency (i.e., 0.50 cpd). However, the amplitude of the energy at 0.50 cpd exceeds the amplitude at 0.25 cpd only when Δ_t is higher than 90°. In other words, for Δ_t of 90° and below, spatial frequency channel centered at 0.25 cpd is stimulated but at higher Δ_t values, spatial frequency channel centered at 0.50 cpd is stimulated.

To identify if this energy shift from nominal to doubled spatial frequency is detrimental to the experiment, it is important to examine the bandwidths of the spatial frequency channels. According to Wilson (1991), spatial frequency bandwidths (full width at half height) decrease as spatial frequency increases. At 0.80 cpd, bandwidth of spatial frequency channel is about 2 octaves but at 2.20 cpd, it is approximately 1.3 octave. Hence, this shift in energy from nominal spatial frequency to doubled spatial frequency can influence our results for the 2.20 cpd stimulus but only when the value of Δ_t is higher than 90°. However, as shown in Figures 5 and 6, our TPD thresholds for the 2.20-cpd grating never approach Δ_t value of 90°. Visual inspection of the stimulus display also confirmed that the apparent brightness was only visible when Δ_t was above threshold. Hence, we are convinced that our results are not influenced by any apparent brightness cue. Mechler and Victor (2000) reported on the apparent motion cue in their stimulus. We modified their stimulus design to avoid the apparent motion cue and simultaneously made the task easier for our subjects. However, these modifications appear to lead to changes in apparent brightness of the composite grating of 2.20 cpd grating at suprathreshold Δ_t values. Thus, it

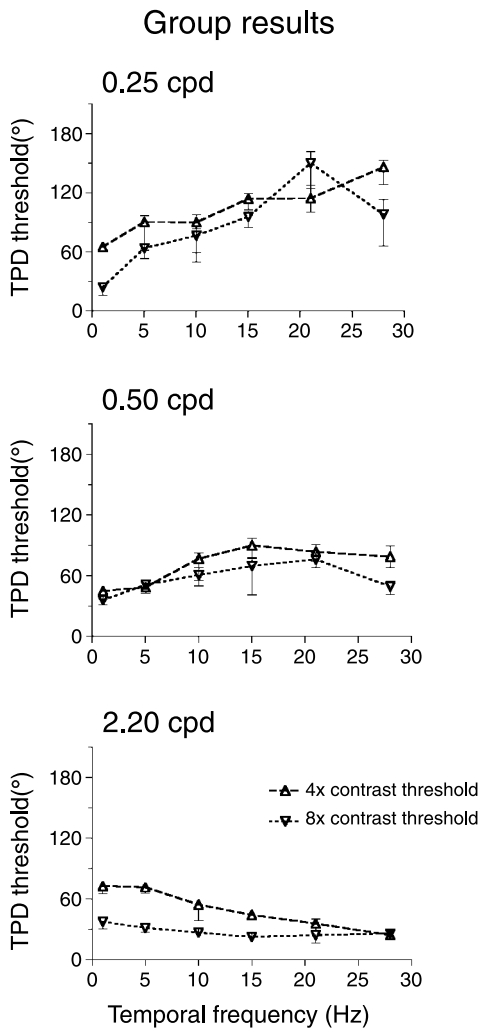

Figure 7. Group results of temporal frequency-dependent TPD thresholds. Results in Figures 3, 4, and 5 are averaged. Error bars are derived from square root of averaging variance of data points.

seems that in this type of temporal comparison tasks it is very difficult to avoid such unwanted visual phenomena.

In conclusion, we agree with White et al. (2002) that the loss of temporal phase encoding could be a possible reason for the perception of doubled spatial frequencies in the FDI. This theory suggests that the doubled frequency in the FDI is actually doubled "in time" not "in space." However, this theory can only explain the perception of doubled spatial frequency, not the greater and less than double increase in apparent periodicity reported by several spatial frequency matching studies (Demirel, Vingrys, Anderson, & Johnson, 1999; Kulikowski, 1975; Maddess & Kulikowski, 1999; McKendrick, Anderson, Johnson, & Fortune, 2003; Parker, 1981; Richards & Felton, 1973). Neither can it explain the results of recent studies which have suggested that the apparent spatial structure in the FDI is not sinusoidal but appears distorted with unequal widths of anti-nodal and nodal regions (Anderson & Johnson, 2002; Vallam, 2006; Vallam & Metha, 2007). Anderson and Johnson (2002) suggests that these changes in the local spatial structure of the FDI could be a result of two opposing mechanisms—a true frequency doubling mechanism that gives the perception of the doubled frequency and a local size encoding mechanism, which alters the apparent spatial structure of the flickering gratings. It is likely that the loss of temporal phase encoding is the true frequency doubling mechanism, while the mechanism described by Anderson and Johnson is the local size encoding mechanism and both these mechanisms are active while perceiving the FDI. These studies do not comment if these two mechanisms are purely independent or influence each other at specific frequencies; only further studies can help us understand more about the interplay between these two mechanisms.

Acknowledgments

Preliminary work for this study was supported by a Kaye Merlin Brutton Award, administered by The University of Melbourne. Kunjam Vallam received support from the David Hay Memorial Fund, The University of Melbourne, Australia.

There are no conflicts of interest regarding this manuscript. We also confirm that this work has not been published elsewhere and is not under review with another journal, and that if published in *Journal of Vision* it will not be reprinted elsewhere in any language in the same form without the consent of the publisher, who holds the copyright.

Commercial relationships: none.
Corresponding author: Andrew B. Metha.
Email: ametha@unimelb.edu.au.
Address: Department of Optometry & Vision Sciences, The University of Melbourne, Cnr. Keppel & Cardigan Streets, Carlton, Victoria 3053, Australia.

References

Anderson, A. J., & Johnson, C. A. (2002). Effect of spatial waveform on apparent spatial frequency. *Vision Research, 42,* 725–732. [PubMed]

Blakemore, C., & Vital-Durand, F. (1986). Organization and post-natal development of the monkey's lateral geniculate nucleus. *The Journal of Physiology, 380,* 453–491. [PubMed] [Article]

Demirel, S., Vingrys, A. J., Anderson, A. J., & Johnson, C. (1999). Spatio-temporal properties of the frequency doubling effect. *Investigative Ophthalmology & Visual Science, 40,* S42.

Derrington, A. M., & Lennie, P. (1984). Spatial and temporal contrast sensitivities of neurones in lateral geniculate nucleus of macaque. *The Journal of Physiology, 357,* 219–240. [PubMed] [Article]

Efron, B., & Tibshirani, R. J. (1998). *An introduction to the Bootstrap*. New York: Chapman & Hall/CRC.

Fahle, M. (1993). Figure-ground discrimination from temporal information. *Proceedings of the Royal Society of London B: Biological Sciences, 254,* 199–203. [PubMed] [Article]

Forte, J., Hogben, J. H., & Ross, J. (1999). Spatial limitations of temporal segmentation. *Vision Research, 39,* 4052–4061. [PubMed]

Kaplan, E., & Shapley, R. M. (1982). X and Y cells in the lateral geniculate nucleus of macaque monkeys. *The Journal of Physiology, 330,* 125–143. [PubMed] [Article]

Kaplan, E., & Shapley, R. M. (1986). The primate retina contains two types of ganglion cells, with high and low contrast sensitivity. *Proceedings of the National Academy of Sciences of the United States of America, 83,* 2755–2757. [PubMed] [Article]

Kelly, D. (1966). Frequency doubling in visual responses. *Journal of the Optical Society of America, 56,* 1628–1633.

Kojima, H. (1998). Figure/ground segregation from temporal delay is best at high spatial frequencies. *Vision Research, 38,* 3729–3734. [PubMed]

Kulikowski, J. J. (1975). Apparent fineness of briefly presented gratings: Balance between movement and pattern channels. *Vision Research, 15,* 673–680. [PubMed]

Lee, S. H., & Blake, R. (1999a). Detection of temporal structure depends on spatial structure. *Vision Research, 39,* 3033–3048. [PubMed]

Lee, S. H., & Blake, R. (1999b). Visual form created solely from temporal structure. *Science, 284,* 1165–1168. [PubMed]

Leonards, U., Singer, W., & Fahle, M. (1996). The influence of temporal phase differences on texture segmentation. *Vision Research, 36,* 2689–2697. [PubMed]

Maddess, T., & Henry, G. H. (1990). Density of non-linear visual units and glaucoma. *Investigative Ophthalmology, 31,* S230.

Maddess, T., & Henry, G. H. (1992). Performance of nonlinear visual units in ocular hypertension and glaucoma. *Clinical Vision Sciences, 7,* 371–383.

Maddess, T., & Kulikowski, J. J. (1999). Apparent fineness of stationary compound gratings. *Vision Research, 39,* 3404–3416. [PubMed]

Marrocco, R. T., McClurkin, J. W., & Young, R. A. (1982). Spatial summation and conduction latency classification of cells of the lateral geniculate nucleus of macaques. *Journal of Neuroscience, 2,* 1275–1291. [PubMed] [Article]

McKendrick, A. M., Anderson, A. J., Johnson, C. A., & Fortune, B. (2003). Appearance of the frequency doubling stimulus in normal subjects and patients with glaucoma. *Investigative Ophthalmology & Visual Science, 44,* 1111–1116. [PubMed] [Article]

Mechler, F., & Victor, J. D. (2000). Comparison of thresholds for high-speed drifting vernier and a matched temporal phase-discrimination task. *Vision Research, 40,* 1839–1855. [PubMed]

Parker, A. (1981). Shifts in perceived periodicity induced by temporal modulation and their influence on the spatial frequency tuning of two aftereffects. *Vision Research, 21,* 1739–1747. [PubMed]

Parker, A. (1983). The effects of temporal modulation on the perceived spatial structure of sine-wave gratings. *Perception, 12,* 663–682. [PubMed]

Richards, W., & Felton, T. B. (1973). Spatial frequency doubling: Retinal or central? *Vision Research, 13,* 2129–2137. [PubMed]

Rogers-Ramachandran, D. C., & Ramachandran, V. S. (1998). Psychophysical evidence for boundary and surface systems in human vision. *Vision Research, 38,* 71–77. [PubMed]

Shapley, R., Kaplan, E., & Soodak, R. (1981). Spatial summation and contrast sensitivity of X and Y cells in the lateral geniculate nucleus of the macaque. *Nature, 292,* 543–545. [PubMed]

Vallam, K. (2006). Psychophysical explorations of the illusion underpinning frequency doubling perimetry in glaucoma. Unpublished PhD dissertation, The University of Melbourne, Melbourne.

Vallam, K., & Metha, A. B. (2007). Spatial structure of the frequency doubling illusion. *Vision Research, 47,* 1732–1744. [PubMed]

Victor, J. D., & Conte, M. M. (2002). Temporal phase discrimination depends critically on separation. *Vision Research, 42,* 2063–2071. [PubMed]

White, A. J., Sun, H., Swanson, W. H., & Lee, B. B. (2002). An examination of physiological mechanisms underlying the frequency-doubling illusion. *Investigative Ophthalmology & Visual Science, 43,* 3590–3599. [PubMed] [Article]

Wilson, H. R. (1991). Psychophysical models of spatial vision and hyperacuity. In D. Regan (Ed.), *Spatial vision* (vol. 10). The Macmillan Press Ltd.